Frontiers of Information Technology & Electronic Engineering
www.zju.edu.cn/jzus; engineering.cae.cn; www.springerlink.com
ISSN 2095-9184 (print); ISSN 2095-9230 (online)
E-mail: jzus@zju.edu.cn

Carbon emission impact on the operation of virtual power plant with combined heat and power system

Yu-hang XIA[†1], Jun-yong LIU[1], Zheng-wen HUANG[2], Xu ZHANG[3]

([1]*School of Electrical Engineering and Information, Sichuan University, Chengdu 610065, China*)

([2]*Brunel Institute of Power Systems, Brunel University, London UB8 3PH, UK*)

([3]*Guangzhou Power Supply Bureau, Guangzhou 510000, China*)

[†]E-mail: scxyh@foxmail.com

Received Dec. 22, 2015; Revision accepted Mar. 10, 2016; Crosschecked Apr. 14, 2016

Abstract: A virtual power plant (VPP) can realize the aggregation of distributed generation in a certain region, and represent distributed generation to participate in the power market of the main grid. With the expansion of VPPs and ever-growing heat demand of consumers, managing the effect of fluctuations in the amount of available renewable resources on the operation of VPPs and maintaining an economical supply of electric power and heat energy to users have been important issues. This paper proposes the allocation of an electric boiler to realize wind power directly converted for supplying heat, which can not only overcome the limitation of heat output from a combined heat and power (CHP) unit, but also reduce carbon emissions from a VPP. After the electric boiler is considered in the VPP operation model of the combined heat and power system, a multi-objective model is built, which includes the costs of carbon emissions, total operation of the VPP and the electricity traded between the VPP and the main grid. The model is solved by the CPLEX package using the fuzzy membership function in Matlab, and a case study is presented. The power output of each unit in the case study is analyzed under four scenarios. The results show that after carbon emission is taken into account, the output of low carbon units is significantly increased, and the allocation of an electric boiler can facilitate the maximum absorption of renewable energy, which also reduces carbon emissions from the VPP.

Key words: Virtual power plant (VPP), Carbon emissions, Electric boiler, Wind power, Combined heat and power (CHP)
http://dx.doi.org/10.1631/FITEE.1500467 **CLC number:** TM732

1 Introduction

Nowadays, more and more wind turbine, photovoltaic, and energy storage systems are being installed. It is estimated that renewable energy will become the main energy source for global power generation by 2030, accounting for 33% of the world's total generating capacity (Guan *et al.*, 2008).

Installation of a large number of distributed generation units in a distribution network not only reduces the power loss and balances the end-users' load demand, but also changes the direction of power flow in the distribution network (Ackermann *et al.*, 2001; Driesen and Katiraei, 2008). At this stage, however, the allocation of distributed generation is focused only on the connection to the distribution network, where the capacity and location of distributed generation are calculated according to the size of the network. Under this model, the system operator cannot effectively manage a large amount of mini-sized distributed generation. This means that distributed generation cannot supply the necessary energy services when critical situations occur on the main grid, and the system still needs traditional generating units to provide necessary ancillary services (Mohd *et al.*, 2008). This leads to sharp increases in investment and operational costs, and ultimately affects the integration of distributed generation.

ORCID: Yu-hang XIA, http://orcid.org/0000-0002-4586-4537

To facilitate flexible access of various distributed generators to a distribution network, the concept of virtual power plant (VPP) (Kieny *et al.*, 2009; Raab *et al.*, 2011; Saboori *et al.*, 2011) was developed. A VPP can gather together different types of distributed generation in a certain region through the internal communication and control architecture (Mashhour *et al.*, 2011; Pandžić *et al.*, 2013) to smooth the electric power generation. This allows micro distributed generation to participate in energy market transactions (Lombardi *et al.*, 2011; Hernandez *et al.*, 2013; Xia and Liu, 2016a). But when a VPP has made unit commitment to market trading, security constraints should be satisfied by analyzing the injected power flow in each bus node, so each distributed generator could participate in electric power transaction with their scheduled output (Xia and Liu, 2016b). To realize the management of controllable load in VPPs, a load control algorithm was proposed, which makes the controllable load benefit from power market transaction, and reduced network loss and congestion in VPPs (Ruiz *et al.*, 2009). From the above literature analysis, it would appear that the users' electric power demand is the only factor considered in VPP operations. However, consumers in a VPP also have a certain amount of heat demand (especially in winter). The ability of a VPP to supply heat for users would be greatly restricted under the fixing heat process of combined heat and power (CHP) units. This means that conventional distribution generation in VPPs has to start up during peak heat demand, causing wind power curtailment (Ummels *et al.*, 2007). A case in Denmark was used to investigate the ability of VPPs to facilitate wind power absorption. This case showed that surplus wind power can not only provide electricity and heat for domestic customers, but also increase the profitability of VPPs (Wille-Haussmann *et al.*, 2010). The amount of carbon emitted during the process of the VPP providing heat for users is a very important factor that needs to be considered. Because of the existence of a carbon emission market, the controllability of carbon emissions will have a significant impact on VPP operations (Skarvelis-Kazakos *et al.*, 2013). Therefore, the influence of operating costs and emissions of CO_2 and NO_X on the formation of a VPP has been discussed (Arslan and Karasan, 2013).

Because of the complementary relationship between wind power and consumers' heat demand (Lund and Münster, 2003), this paper proposes the idea of allocating electric boilers to VPPs. This could make use of wind power to generate heat for users, and compensate for the reduced real power because of the decreasing heat output of CHP units. Also, because of the flexible operation of electric boilers, this could effectively reduce the frequent start-up of conventional units in VPPs caused by the fluctuation of renewable distributed generation output, and maximize the use of wind power, photovoltaic and other renewable distributed generation.

2 Virtual power plant structure

Fig. 1 shows a typical VPP comprising a micro CHP generation unit (μCHP), a micro wind turbine, a photovoltaic (PV) system, a micro conventional distributed generation, storage system (including energy and heat), and the controllable load. Because a VPP is an open system, the fluctuation level of the wind turbine and PV output will affect its operation and profit. For example, when the power output of a VPP surpasses the internal load demand, it can make an electricity transaction in the main grid power market (P_{exp} in Fig. 1). If there is an energy deficit in the VPP, it can purchase electricity from the main grid through a 'virtual tie line' (P_{imp} in Fig. 1). In addition, the presence of CHP units gives the VPP the ability to

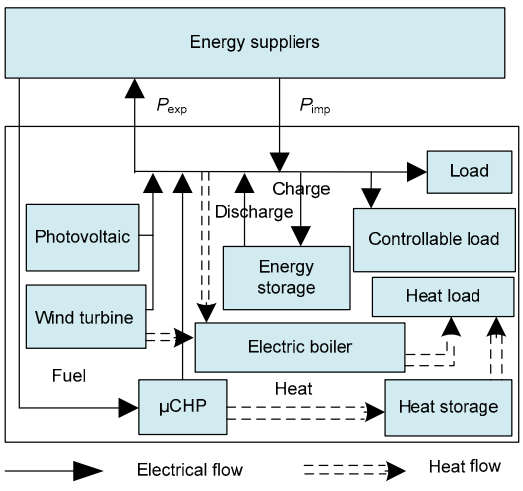

Fig. 1 The structure of a virtual power plant

provide heat demand for internal users, and the presence of an electric boiler obviously improves the utilization rate of wind power.

3 Carbon emission regulation

The main source of carbon emissions in a VPP is the conventional distributed generation, such as micro gas turbines and micro diesel engines. Carbon emission regulation means VPPs can buy or sell the amount of carbon emissions through the legal carbon emissions trading market to control the total carbon emissions in the VPP (Perroni and Rutherford, 1993). This kind of mechanism uses economic means to reduce carbon emissions. After carbon emission regulations were applied to VPPs, the marginal cost of the conventional distributed generation increased, and the consumption of renewable energy in VPPs has been greatly promoted. The cost model of carbon emission in a VPP is as follows:

$$F = p\left(\sum_{t=1}^{T}\sum_{i=1}^{N}\sigma_i P_{G_{i,t}}\Delta T\cdot l_i - \varepsilon\cdot\sum_{t=1}^{T}\gamma P_{D,t}\right), \quad (1)$$

where p denotes the carbon-trade price, σ_i the carbon emission intensity of the ith unit (kg/(kW·h)), $P_{G_{i,t}}$ the power output of the ith unit at the tth hour, ΔT the time interval, l_i the start-up state of the ith unit, ε the load correction parameter of the total hour period, γ the carbon emissions coefficient per unit of power (kg/(kW·h)), $P_{D,t}$ the total power output at the tth hour, T the number of time intervals, and N the number of distributed generations.

4 Problem formulation

4.1 Operation cost model of micro CHP

If the type of the CHP unit and the efficiency of combustion are neglected, the mathematical model of the thermal power system of micro CHP is as follows:

$$Q_{\mathrm{MT}} = P_{\mathrm{CHP}}(1-\eta_{\mathrm{e}}-\eta_{\mathrm{loss}})/\eta_{\mathrm{e}}, \quad (2)$$

$$Q_{\mathrm{he}} = Q_{\mathrm{MT}}K_{\mathrm{he}}, \quad (3)$$

where Q_{MT}, P_{CHP}, η_{e}, and η_{loss} are the amount of exhaust heat, the amount of power generation, power efficiency, and the heat loss coefficient of the gas turbine of the CHP units, respectively. Q_{he} is the amount of heat provided by the exhaust gas of the CHP unit and K_{he} the heating coefficient.

The fuel cost of micro CHP is as follows:

$$C_{\mathrm{MT}} = \rho_{\mathrm{gas}}\sum_{t=1}^{T}\frac{P_{\mathrm{CHP}}}{9.7\eta_{\mathrm{e}}}, \quad (4)$$

where 9.7 is the calorific value of natural gas (kW·h/m^3), ρ_{gas} the natural gas price (CNY/m^3), and C_{MT} the fuel cost of the CHP unit.

4.2 Profit model for wind power consumption in a virtual power plant

Part of the wind power is used to run the electric boiler, which generates heat for users in the VPP (Fig. 2). The rest of the wind power is used to compensate for the reduced power output of CHP units. The combined use of a wind turbine and electric boiler can not only increase the utilization rate of wind power, but also reduce the carbon emissions and operation costs of CHP units.

Thus, the relationship among the output of CHP units, electric boilers, and wind power can be stated as follows:

$$\begin{cases}\Delta P_{\mathrm{CHP}} = \dfrac{\beta_{\mathrm{EB}}}{\beta_{\mathrm{EB}}+\gamma_{\mathrm{CHP}}}P^{\mathrm{w}},\\ P_{\mathrm{EB}} = \dfrac{\gamma_{\mathrm{CHP}}}{\beta_{\mathrm{EB}}+\gamma_{\mathrm{CHP}}}P^{\mathrm{w}},\end{cases} \quad (5)$$

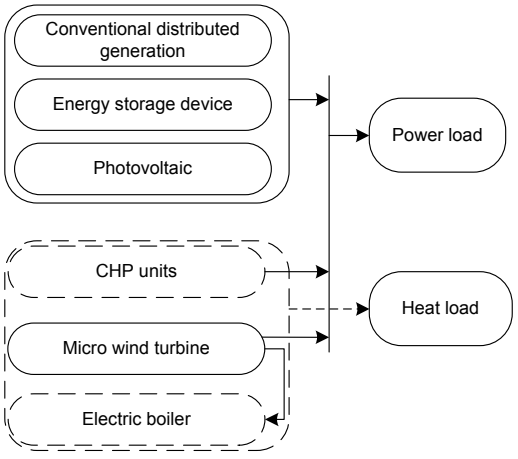

Fig. 2 Wind power consumption in the virtual power plant

where β_{EB}, γ_{CHP}, P^{w}, ΔP_{CHP}, and P_{EB} are the heat production efficiency of the electric boiler, heat-to-electric ratio, wind power output, reduced real power of the CHP unit, and power consumption of the electric boiler, respectively.

Under a given thermal efficiency of CHP units, l_{CHP}, the volume of natural gas consumed for a gas turbine to generate a unit quantity of electricity, is expressed as follows:

$$l_{CHP}=\frac{\gamma_{CHP}+1}{9.7\beta_{CHP}}, \tag{6}$$

where β_{CHP} is the fuel utilization efficiency of the CHP unit.

In this study, β_{EB} is defined as 1, and the value of the heat-to-electric ratio, γ_{CHP}, is 1.5. According to Eqs. (5) and (6), when the absorptive power for electric boilers is P_{EB}, the saving in the volume of natural gas, L_{CHP}, can be stated as follows:

$$\begin{aligned}L_{CHP}&=\Delta P_{CHP}\cdot l_{CHP}\\&=\frac{0.104\beta_{EB}(1+\gamma_{CHP})}{\beta_{CHP}(\beta_{EB}+\gamma_{CHP})}P^{w}=\frac{0.104}{\beta_{CHP}}P^{w}.\end{aligned} \tag{7}$$

According to Eq. (7), the profit from wind power consumption in the VPP can be expressed as

$$f_{w}=\rho_{gas}L_{CHP}+\rho_{el}\Delta P_{CHP}, \tag{8}$$

where ρ_{gas} is the retail price of natural gas (CNY/m^3), ρ_{el} the retail electricity price in the VPP (CNY/kW), and L_{CHP} the saving amount of natural gas.

4.3 Operation model combining heat and power of the VPP considering carbon emissions

4.3.1 Objective function

In this study, the power output of distributed generation in the VPP per hour and the operation states of the units are taken as the decision variables, and the power network and unit characteristics are taken as the constraint conditions. So, an objective function including the costs of the overall operation of the VPP, carbon emissions, and traded electricity, is established as follows:

1. The cost of carbon emissions (sub-objective function 1) is

$$\min f_1=\min p\left(\sum_{t=1}^{T}\sum_{i=1}^{N}\sigma_i P_{G_{i,t}}\Delta T\cdot l_i-\varepsilon\cdot\sum_{t=1}^{T}\gamma P_{D,t}\right). \tag{9}$$

2. The operation cost of combined power and heat of the VPP (sub-objective function 2) is

$$\begin{aligned}\min f_2=\min\sum_{t=1}^{T}\Bigg(&\sum_{i=1}^{N_{DG}}(f_i(P_{i,t}^{t})+S_{i,t}^{U}+S_{i,t}^{D})-f_{w}\\&+\sum_{j=1}^{N_{CHP}}f_j(P_{j,t}^{CHP},H_{j,t}^{CHP})+\sum_{k=1}^{N_{STR}}f_k(P_{k,t}^{STR})\Bigg),\end{aligned} \tag{10}$$

where $P_{i,t}^{t}$, $S_{i,t}^{U}$, and $S_{i,t}^{D}$ are the power output, start-up cost, and shut-down cost of the ith conventional unit in the VPP at time interval t, respectively, $P_{j,t}^{CHP}$ and $H_{j,t}^{CHP}$ are the electricity and heat output of the jth CHP unit at time interval t, respectively, $P_{k,t}^{STR}$ is the power output of the kth storage system at time interval t, and N_{DG}, N_{CHP}, and N_{STR} are the numbers of conventional units, CHP units, and storage systems, respectively.

3. Cost of electricity traded between the VPP and the main grid (sub-objective function 3)

Due to the fluctuation characteristics of distributed renewable energy generation outputs, the VPP makes electricity transactions with the main grid through a 'virtual tie line'. Therefore, the traded electricity cost can be stated as follows:

$$\min f_3=\min\sum_{t=1}^{24}[\alpha_t x_{\alpha}(t)-\beta_t x_{\beta}(t)]P_{m}(t), \tag{11}$$

where $x_{\alpha}(t)$ and $x_{\beta}(t)$ are the state variables of power purchase and power selling of the VPP at time interval t, respectively, α_t and β_t are the power purchase price from the main grid and power selling price to the main grid, respectively, and $P_m(t)$ is the traded electricity between the VPP and the main grid. If $P_m(t)<0$, $x_{\alpha}(t)=1$, or if $P_m(t)>0$, $x_{\beta}(t)=1$, restrained as follows:

$$\begin{cases}x_k(t)\in\{0,1\},\ k\in\{\alpha,\beta\},\\ x_{\alpha}(t)+x_{\beta}(t)\le 1.\end{cases} \tag{12}$$

Therefore, the proposed multi-objective function can be expressed as

$$\min f = \min(f_1, f_2, f_3). \tag{13}$$

4.3.2 Constraints

1. Internal constraints of the VPP

(1) The power balance equation under the condition of neglect of network loss is

$$P_{\mathrm{m}}(t) + \sum_{i=1}^{N_{\mathrm{STR}}} P_{i,t}^{\mathrm{STR}} + \sum_{i=1}^{N_{\mathrm{CHP}}} (P_{i,t}^{\mathrm{CHP}} - \Delta P_{\mathrm{CHP},t}) + \sum_{i=1}^{N_{\mathrm{DG}}} P_{i,t} = P_{\mathrm{load},t}. \tag{14}$$

(2) The heat balance equation is

$$\sum_{i=1}^{T} P_{\mathrm{EB},t} + \sum_{i=1}^{N_{\mathrm{CHP}}} Q_{i,t}^{\mathrm{CHP}} + \sum_{i=1}^{N_{\mathrm{STR}}} Q_{i,t}^{\mathrm{STR}} = Q_t. \tag{15}$$

2. Constraints of CHP units

The operating range of the CHP is described by a series of linear inequality constraints. If the operating range of the ith CHP unit has N_i inequality constraints, then

$$\begin{cases} \alpha_1 P_{i,t}^{\mathrm{CHP}} + \beta_1 Q_{i,t}^{\mathrm{CHP}} \le \gamma_1, \\ \alpha_2 P_{i,t}^{\mathrm{CHP}} + \beta_2 Q_{i,t}^{\mathrm{CHP}} \le \gamma_2, \\ \quad\quad ... \\ \alpha_{N_i} P_{i,t}^{\mathrm{CHP}} + \beta_{N_i} Q_{i,t}^{\mathrm{CHP}} \le \gamma_{N_i}, \end{cases} \tag{16}$$

where α_1–α_{N_i}, β_1–β_{N_i}, and γ_1–γ_{N_i} are the inequality constraint coefficients of the operating range of the ith CHP unit.

3. Constraints of the electric boiler

An electric boiler usually uses electric resistance wire for electric heat conversion, so the power output constraints of the ith electric boiler are

$$\begin{cases} Q_{i,t}^{\mathrm{EB}} = \beta_{\mathrm{EB}} P_{i,t}^{\mathrm{EB}}, \\ 0 \le P_{i,t}^{\mathrm{EB}} \le \overline{P}_{i,t}^{\mathrm{EB}}, \end{cases} \tag{17}$$

where $P_{i,t}^{\mathrm{EB}}$, $Q_{i,t}^{\mathrm{EB}}$, and $\overline{P}_{i,t}^{\mathrm{EB}}$ are the electric power, heating power, and rated electric power, respectively.

4. Other constraints

These include the power output constraints of the conventional distributed generation, energy storage device, and the corresponding ramp rate of units, which have been described in detail by Pudjianto *et al.* (2007) and Teleke *et al.* (2009).

4.4 Model solving

In this study, the operation period of the VPP is 24 h, and the wind turbine, photovoltaic and other renewable distributed generation are under maximum power tracking mode to use renewable energy as much as possible. When the electric boiler is added to the VPP, the CHP unit will no longer follow the changes in heat load. After the cost function of the unit's operation is expressed by piecewise linearization, the model is solved using the CPLEX package in Matlab. Because CPLEX cannot solve the multi-objective optimization problem, this model is transformed into a single-objective optimization problem. The expectation value of each sub-objective function has only an upper bound, so the drop-semi-shaped membership function (Bezdek, 1981) in fuzzy mathematics is introduced to deal with three sub-objective functions with fuzzy processing. The membership function of u_i is defined as follows:

$$u_i = \begin{cases} 1, & f_i \le f_{\min,i}, \\ \exp\left(-\dfrac{f_i - f_{\min,i}}{f_{\min,i}}\right), & f_i > f_{\min,i}, \end{cases} \tag{18}$$

where i is 1, 2, or 3, and $f_{\min,i}$ can be the minimum carbon emissions cost, the minimum operating cost, or the minimum traded electricity cost if the objective function i satisfies the respective constraints. With the introduction of the membership function, the multi-objective function is transformed into a single-objective problem, which can satisfy the nonlinear constraints. Thus, the degree of membership of the multi-objective function can be expressed by the largest membership function selected from three membership functions, i.e., u=max(u_1, u_2, u_3). According to Eqs. (14)–(17), the optimization operation model can be transformed as follows:

$$\max u \ \text{ s.t. } u \le u_i \text{ and } 0 < u \le 1. \tag{19}$$

5 Case study

The VPP structure is shown in Fig. 3, where power load 1 is residential load, power load 2 is commercial load, and power loads 3–5 are industrial loads. The total power load and heat load, and the

output curve predicted from wind turbine and photovoltaic power are shown in Fig. 4. The carbon emission quota per unit of electricity in the VPP is 0.56 kg/(kW·h) and the carbon trading price is 0.12 CNY/kg. Parameter β_{CHP} is 0.9, η_e is 0.4, the heating efficiency is 0.6, and η_{loss} is 0.15. The price of natural gas is 2.5 CNY/m^3. The electricity price data in the VPP are taken from Li *et al.* (2015) and the capacity limit of the 'virtual tie line' is 80 kW. The operating parameters of units in the VPP are shown in Table 1.

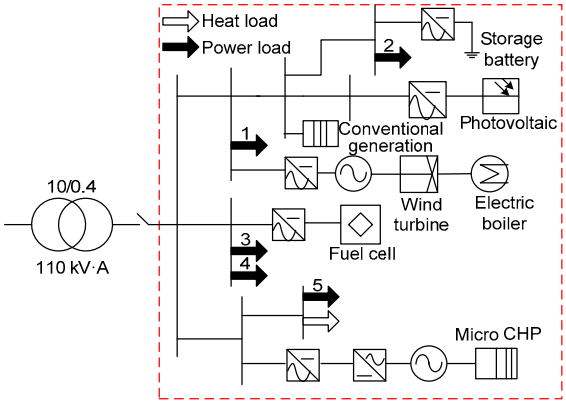

Fig. 3 Diagram of the virtual power plant

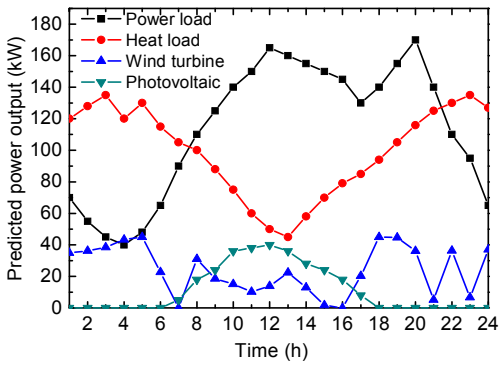

Fig. 4 Curves of the predicted output of photovoltaic, wind energy generation, and the load profile

5.1 Scenario analysis

To study the influence of the carbon emissions and the allocation of the electric boiler on the VPP operation, the total operating cost of the VPP and unit output in the VPP are analyzed under four scenarios.

Scenario A (Operation of the VPP without considering the allocation of an electric boiler or carbon emissions) Without the allocation of electric boilers, the CHP unit in the VPP has to follow the change in heat demand, which makes the output curve of the CHP unit very similar to the heat demand curve (Fig. 5). Without the carbon emission constraint, the output curve of the conventional unit is also very similar to the power demand curve. This is because the operational cost of the conventional unit is lower than that of the fuel cell units, which makes the conventional units be the main power source supplying electrical energy. As for the storage battery, it is

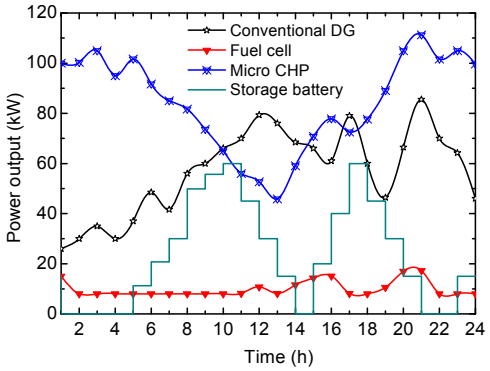

Fig. 5 Operation of the virtual power plant under scenario A

Table 1 The parameters of units in the virtual power plant

Component	P_{max} (kW)	P_{min} (kW)	R_{up} (kW)	R_{down} (kW)	H_{max} (kW)	H_{min} (kW)	σ	a	b	c
Conventional DG	150	8	20	20	–	–	0.83	0.15	8.5	15
Fuel cell	150	8	20	20	–	–	0.25	0.20	10.5	15
Micro CHP	80	15	20	20	180	–	0.90	0.15	9.0	10
Storage battery	60	0	15	15	–	–	–	0.05	6.0	5
Photovoltaic	40	0	–	–	–	–	–	–	–	–
Wind turbine	45	0	–	–	–	–	–	–	–	–

P_{max}: the maximum output power of the generation unit; P_{min}: the minimum output power of the generation unit; R_{up}: ramp up reserve of the generation unit per hour; R_{down}: ramp down reserve of the generation unit per hour; H_{max}: the maximum output heat of the CHP unit; H_{min}: the minimum output heat of the CHP unit; σ: carbon emission intensity of the generation unit; a, b, and c: coefficients of the generation unit operation. DG: distributed generation; CHP: combined heat and power unit

charging from hour 5 to hour 11, which means the total output of units is more than the load profile, so the surplus energy can be used to charge the battery. But from hour 12 to hour 14, because of the peak load demand and the economical efficiency of the storage battery, the battery starts to discharge for load in the VPP, which makes conventional units ramp down. From hour 15 to hour 18, because of the low power price of flat load during this time, the VPP decides to charge the battery instead of selling electrical energy to the main grid. This energy can be used to curtail the peak load amount from hour 18 to hour 21. This can reduce the total cost of the VPP and the electricity purchased from the main grid during peak load demand.

Scenario B (Operation of the VPP under carbon emission constraints without the allocation of the electric boiler) With carbon emission constraints in the VPP, the conventional unit is replaced by the fuel cell as the main power source, even with its higher operational cost (Fig. 6). The power output of the conventional unit is around 40 kW at hours 13 and 21 (peak load profile). At other time intervals, the conventional unit maintains minimum power output because of low load demand. The storage battery is used mainly to supply energy with fuel cell in scenario B because of no carbon emissions, and the charging state of the battery is obviously less than that in scenario A.

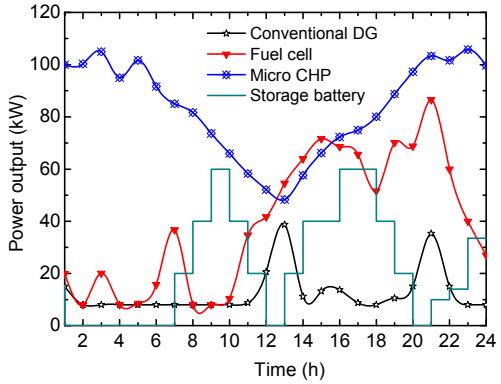

Fig. 6 Operation of the virtual power plant under scenario B

Scenario C (Operation of the VPP with the electric boiler but without considering carbon emissions) After the electric boiler is allocated to the VPP, the CHP unit could no longer follow the changing trend in heat demand (Fig. 7). The deficit in heat demand could be supplied jointly by wind and conventional units, in which electrical power is converted to heat with about 100% efficiency. This achieves full use of wind power (Fig. 7). The output power curves of the CHP units and fuel cell are very flat compared to the curves in Figs. 5 and 6, and the battery is charging at most of the time in a day. Only at hour 13 is the battery fully discharged. The capacity of the battery is very similar to the output curve of wind power and photovoltaic in the VPP, which shows that the allocation of the electric boiler to a VPP can improve the utilization ratio of renewable energy.

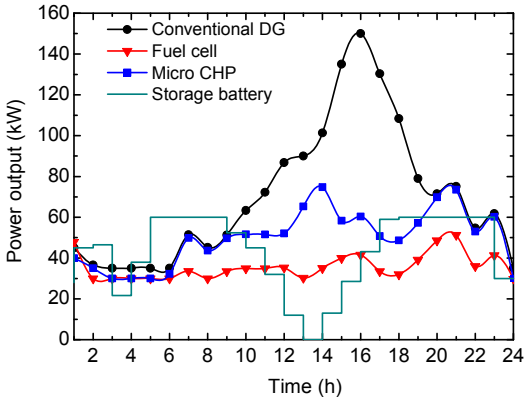

Fig. 7 Operation of the virtual power plant under scenario C

Scenario D (Operation of the VPP with the electric boiler and considering carbon emissions) When the carbon emission constraint is included in the operation of the VPP, the power output of fuel cell bumps up instantly, while the output of the conventional unit is forced to ramp down. Because the heat demand gap led by the reduction in the output of the CHP unit is compensated by the joint operation of the fuel cell and electric boiler (Fig. 8), the lowest point in the output curve of the fuel cell is at hour 13 (37.64 kW). From hour 16 to hour 21, the output of the fuel cell gradually increases from 110.24 kW to 148.69 kW, which is consistent with the electric load demand curve. Similarly, to reduce the overall carbon emissions in the VPP, the power curve of the battery is in a discharged state from hour 6 to hour 13, because the wind power is zero at hour 14, and the VPP does not charge the battery. From the start of hour 16, wind power increases and there is surplus electricity in the VPP, so

the battery starts to charge, maintaining the maximum capacity.

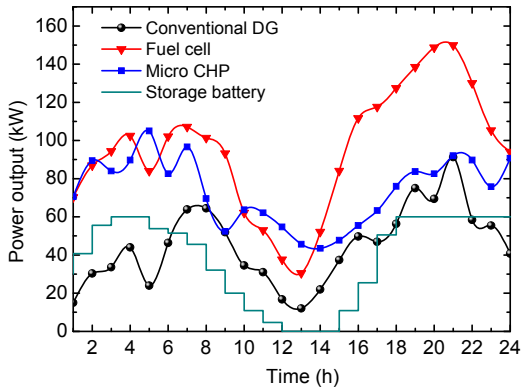

Fig. 8 Operation of the virtual power plant under scenario D

5.2 Analysis of the amount of traded electricity under different scenarios

Without considering carbon emission constraints, the amount of traded electricity in scenario C reaches 324.63 kW in total (Fig. 9). Due to the operational flexibility of the VPP with the allocation of the electric boiler, there is more surplus energy in the VPP to participate in the main power market. Because of the low electricity price in the valley of load demand, such as at hours 1–5 and 22–24, buying electricity from the main grid would be an economic way to balance the load profile instead of ramping up units, so the traded electricity is negative. Compared to scenario C, the traded electricity in scenario A is only 240.07 kW in total, and the maximum traded electricity capacity (63.15 kW) is at hour 17, because of the energy load valley and lower heat demand. As for other time intervals, the CHP units have to follow the changing trend in heat demand, and other units have to balance the load profile as much as possible, so the traded electricity is around zero. The amount of traded electricity is 206.35 kW in scenario B and 229.95 kW in scenario D, which clearly shows the advantage of allocating the electric boiler to the VPP.

5.3 Analysis of carbon emissions under different scenarios

There is a significant difference in carbon emissions between scenarios A and D, which are the extreme scenarios in the case study (Fig. 10). The total amount of carbon emitted in scenario A is 2963.78 kg, but in scenario D, this has decreased by 24.53% to 2236.76 kg. The amount of carbon emitted is 2597.14 kg in scenario B and 2903.94 kg in scenario C. Fig. 10 shows that the allocation of the electric boiler reduces the carbon emissions of the VPP.

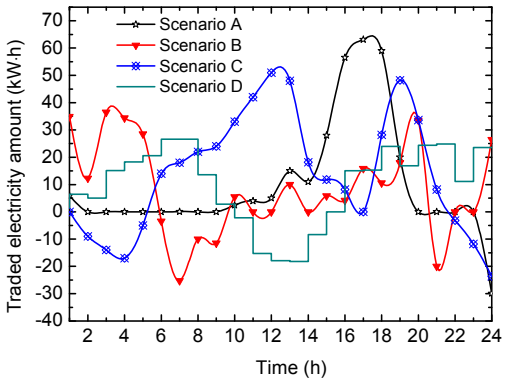

Fig. 9 Traded electricity between the virtual power plant and the main grid under different scenarios

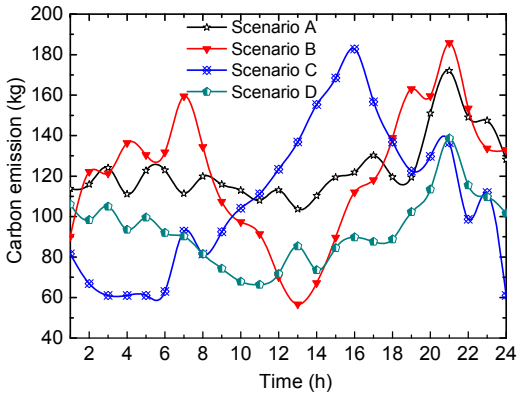

Fig. 10 The amount of carbon emitted under different scenarios

5.4 Analysis of single- and multi-objective optimization results

To investigate the effect of carbon emission constraints on the operation of the VPP with an electric boiler, the calculation results of scenarios C and D are compared (Tables 2 and 3).

Tables 2 and 3 show that if the overall operational cost of a VPP is the only factor to be considered in the two scenarios, the VPP will place the main emphasis on units with lower operational cost, such as the conventional unit and storage battery. Because of the limited capacity of the storage battery, the VPP

Table 2 Single- and multi-objective optimization results in scenario C

Item	f_2 (CNY)	f_3 (CNY)	f (CNY)	Carbon emission (kg)
Operation cost of VPP	24311.49	1586.48	25897.97	1624.45
Traded electricity cost	38212.77	752.20	38964.97	3249.97
Multi-objective optimization	29874.44	1204.24	31078.68	2903.94

f_2: sub-objective function 2; f_3: sub-objective function 3; f: the proposed multi-objective function

Table 3 Single- and multi-objective optimization results in scenario D

Item	f_2 (CNY)	f_3 (CNY)	f (CNY)	Carbon emission (kg)
Operation cost of VPP	24253.39	1806.38	26059.77	1051.19
Traded electricity cost	35445.26	1452.20	36897.46	2749.97
Multi-objective optimization	31968.52	1945.86	33914.38	2236.76

f_2: sub-objective function 2; f_3: sub-objective function 3; f: the proposed multi-objective function

has to buy more electric energy from the main grid during the low load time, which increases the cost of traded electricity. To minimize the cost of traded electricity, the VPP will turn on the conventional unit to balance the load, which in turn increases carbon emissions in the VPP. Comparing the multi-objective calculation results in Tables 2 and 3, after the carbon emissions from the VPP are taken into consideration, the operational cost of the VPP and the traded electricity cost are increased by 2094.08 and 741.62 CNY, respectively. However, the amount of carbon emitted in scenario D is reduced by 666.98 kg, because when the carbon emission constraints are taken into consideration, low-carbon units in the VPP, such as the fuel cell and storage battery, will be the main power source. Therefore, the power outputs of the conventional unit and CHP unit are greatly reduced, forcing the VPP to purchase more electric energy from the main grid.

6 Conclusions

To promote the consumption of wind power, photovoltaic power, and other renewable energy sources in a VPP, the idea of transferring wind power into heat energy was proposed, and the electric boiler to supply heat for consumers in the VPP was used. Numerical simulation showed that the overall carbon emission of the VPP can be significantly reduced by the introduction of carbon emission constraints and the installation of the electric boiler in the VPP. Also, the allocation of the electric boiler can decouple the production process of heat-electric energy, which maximizes the use of renewable energy and reduces the operational cost of the VPP. In the future, the key research direction about the VPP will focus on coordinating the operation of different energy systems, optimizing energy system configuration under a wide scope of time and space.

References

Ackermann, T., Andersson, G., Söder, L., 2001. Distributed generation: a definition. *Electr. Power Syst. Res.*, **57**(3):195-204. http://dx.doi.org/10.1016/S0378-7796(01)00101-8

Arslan, O., Karasan, O.E., 2013. Cost and emission impacts of virtual power plant formation in plug-in hybrid electric vehicle penetrated networks. *Energy*, **60**:116-124. http://dx.doi.org/10.1016/j.energy.2013.08.039

Bezdek, J.C., 1981. Pattern Recognition with Fuzzy Objective Function Algorithms. Springer-Verlag, New York, USA, p.155-192. http://dx.doi.org/10.1007/978-1-4757-0450-1

Driesen, J., Katiraei, F., 2008. Design for distributed energy resources. *IEEE Power Energy Mag.*, **6**(3):30-40. http://dx.doi.org/10.1109/MPE.2008.918703

Guan, D., Hubacek, K., Weber, C.L., *et al.*, 2008. The drivers of Chinese CO_2 emissions from 1980 to 2030. *Glob. Environ. Change*, **18**(4):626-634. http://dx.doi.org/10.1016/j.gloenvcha.2008.08.001

Hernandez, L., Baladron, C., Aguiar, J.M., *et al.*, 2013. A multi-agent system architecture for smart grid management and forecasting of energy demand in virtual power plants. *IEEE Commun. Mag.*, **51**(1):106-113. http://dx.doi.org/10.1109/MCOM.2013.6400446

Kieny, C., Berseneff, B., Hadjsaid, N., *et al.*, 2009. On the concept and the interest of virtual power plant: some results from the European project Fenix. Proc. IEEE Power & Energy Society General Meeting, p.1-6. http://dx.doi.org/10.1109/PES.2009.5275526

Li, Z.M., Zhang, F., Liang, J., *et al.*, 2015. Optimization on microgrid with combined heat and power system. *Proc.*

CSEE, **35**(14):3569-3576 (in Chinese). http://dx.doi.org/10.13334/j.0258-8013.pcsee.2015.14.011

Lombardi, P., Stötzer, M., Styczynski, Z., *et al.*, 2011. Multi-criteria optimization of an energy storage system within a Virtual Power Plant architecture. Proc. IEEE Power and Energy Society General Meeting, p.1-6. http://dx.doi.org/10.1109/PES.2011.6039347

Lund, H., Münster, E., 2003. Modelling of energy systems with a high percentage of CHP and wind power. *Renew. Energy*, **28**(14):2179-2193. http://dx.doi.org/10.1016/S0960-1481(03)00125-3

Mashhour, E., Moghaddas-Tafreshi, S.M., 2011. Bidding strategy of virtual power plant for participating in energy and spinning reserve markets—Part II: numerical analysis. *IEEE Trans. Power Syst.*, **26**(2):957-964. http://dx.doi.org/10.1109/TPWRS.2010.2070883

Mohd, A., Ortjohann, E., Schmelter, A., *et al.*, 2008. Challenges in integrating distributed energy storage systems into future smart grid. Proc. IEEE Int. Symp. on Industrial Electronics, p.1627-1632. http://dx.doi.org/10.1109/ISIE.2008.4676896

Pandžić, H., Kuzle, I., Capuder, T., 2013. Virtual power plant mid-term dispatch optimization. *Appl. Energy*, **101**:134-141. http://dx.doi.org/10.1016/j.apenergy.2012.05.039

Perroni, C., Rutherford, T.F., 1993. International trade in carbon emission rights and basic materials: general equilibrium calculations for 2020. *Scand. J. Econ.*, **95**(3):257-278. http://dx.doi.org/10.2307/3440355

Pudjianto, D., Ramsay, C., Strbac, G., 2007. Virtual power plant and system integration of distributed energy resources. *IET Renew. Power Gener.*, **1**(1):10-16. http://dx.doi.org/10.1049/iet-rpg:20060023

Raab, A.F., Ferdowsi, M., Karfopoulos, E., *et al.*, 2011. Virtual power plant control concepts with electric vehicles. Proc. 16th Int. Conf. on Intelligent System Application to Power Systems, p.1-6. http://dx.doi.org/10.1109/ISAP.2011.6082214

Ruiz, N., Cobelo, I., Oyarzabal, J., 2009. A direct load control model for virtual power plant management. *IEEE Trans. Power Syst.*, **24**(2):959-966. http://dx.doi.org/10.1109/TPWRS.2009.2016607

Saboori, H., Mohammadi, M., Taghe, R., 2011. Virtual power plant (VPP), definition, concept, components and types. Proc. Asia-Pacific Power and Energy Engineering Conf., p.1-4. http://dx.doi.org/10.1109/APPEEC.2011.5749026

Skarvelis-Kazakos, S., Rikos, E., Kolentini, E., *et al.*, 2013. Implementing agent-based emissions trading for controlling Virtual Power Plant emissions. *Electr. Power Syst. Res.*, **102**:1-7. http://dx.doi.org/10.1016/j.epsr.2013.04.004

Teleke, S., Baran, M.E., Huang, A.Q., *et al.*, 2009. Control strategies for battery energy storage for wind farm dispatching. *IEEE Trans. Energy Conv.*, **24**(3):725-732. http://dx.doi.org/10.1109/TEC.2009.2016000

Ummels, B.C., Gibescu, M., Pelgrum, E., *et al.*, 2007. Impacts of wind power on thermal generation unit commitment and dispatch. *IEEE Trans. Energy Conv.*, **22**(1):44-51. http://dx.doi.org/10.1109/TEC.2006.889616

Wille-Haussmann, B., Erge, T., Wittwer, C., 2010. Decentralised optimisation of cogeneration in virtual power plants. *Solar Energy*, **84**(4):604-611. http://dx.doi.org/10.1016/j.solener.2009.10.009

Xia, Y.H., Liu, J.Y., 2016a. Review of virtual power plant based on distributed generation. *Electr. Power Autom. Equip.*, **36**(4):100-106, 115 (in Chinese). http://dx.doi.org/10.16081/j.issn.1006-6047.2016.04.016

Xia, Y.H., Liu, J.Y., 2016b. Optimal scheduling of virtual power plant with risk management. *J. Power Technol.*, **96**(1):49-56.